Publication III

Frans Vinberg and Ari Koskelainen. 2011. Cobalt (Co^{2+}) can mediate dynamic feedback signals driven by calcium (Ca^{2+}) sensor molecules in mouse rod photoreceptors. Research report. Espoo, Finland: Aalto University, School of Science, Department of Biomedical Engineering and Computational Science. 28 pages. Aalto University publication series SCIENCE + TECHNOLOGY 12/2011. Aalto-ST-12/2011. ISBN 978-952-60-4164-3. ISSN 1799-490X.

Department of Biomedical Engineering and Computational Science (BECS)

Cobalt (Co^{2+}) can mediate dynamic feedback signals driven by calcium (Ca^{2+}) sensor molecules in mouse rod photoreceptors

Frans Vinberg and Ari Koskelainen

Aalto University

SCIENCE + TECHNOLOGY

RESEARCH REPORT

Aalto University publication series
SCIENCE + **TECHNOLOGY** 12/2011

Cobalt (Co^{2+}) can mediate dynamic feedback signals driven by calcium (Ca^{2+}) sensor molecules in mouse rod photoreceptors

F. Vinberg and A. Koskelainen

Aalto University
School of Science
Biomedical Engineering and Computational Science
Biophysics

Aalto University publication series
SCIENCE + **TECHNOLOGY** 12/2011

ISBN 978-952-60-4164-3 (pdf)
ISSN-L 1799-4896
ISSN 1799-490X (pdf)

Aalto Print
Helsinki 2011

Finland

Author
F. Vinberg and A. Koskelainen

Name of the publication
Cobalt (Co^{2+}) can mediate dynamic feedback signals driven by calcium (Ca^{2+}) sensor molecules in mouse rod photoreceptors

Publisher School of Science

Unit Biomedical Engineering and Computational Science (BECS)

Series Aalto University publication series SCIENCE + TECHNOLOGY 12/2011

Field of research Biophysics

Abstract

Calcium (Ca^{2+}) controls negative feedback mechanisms that regulate the sensitivity of the rod photoreceptor cell to light. Ca^{2+} signals are mediated by calcium sensor proteins whose specificity against other ions under a natural cellular environment has rarely been studied. It is clear that these proteins must be very selective against magnesium (Mg^{2+}) since they must function in cells under conditions where [Mg^{2+}] exceeds [Ca^{2+}] by a factor of ~10^4 – 10^5. Mg^{2+} is chemically very similar to Ca^{2+} but significantly smaller, and thus it is expected that also other small divalent cations can be discriminated by Ca^{2+} sensor proteins. We adopted an experimental protocol to study the specificity of the known Ca^{2+} sensor proteins, GCAP and recoverin, against some divalent cations in the intact rod photoreceptor cells with transretinal ERG technique. Surprisingly, we found that the small transition metal ion cobalt (Co^{2+}) can mediate the negative feedback signals that are normally driven by changes in [Ca^{2+}] in the rod outer segment.

Keywords photoreceptor, calcium, cobalt, GCAP, recoverin

ISBN (printed)	**ISBN (pdf)** 978-952-60-4164-3	
ISSN-L 1799-4896	**ISSN (printed)** 1799-4896	**ISSN (pdf)** 1799-490X
Location of publisher Espoo	**Location of printing** Helsinki	**Year** 2011
Pages 4 + 28		

1. Introduction

Calcium (Ca^{2+}) plays an important role in a variety of physiological processes, such as visual transduction, muscle contraction, gene transcription, synaptic transmission and gap junction or ion channel conductance modulation. The ability of the simple ion, Ca^{2+}, to regulate complicated cellular processes is achieved by exact control of intracellular calcium concentration ($[Ca^{2+}]_i$) both in space and time. Inside cells the Ca^{2+} signals are generally mediated by a range of calcium sensor proteins, whose structure and functional properties are modulated by selective binding of calcium to specific binding sites.

For calcium signaling to be fast and effective, $[Ca^{2+}]_i$ should be kept low by well-balanced, rapid inflow and extrusion of calcium ions. The low $[Ca^{2+}]_i$, however, poses high demands on the selectivity of the calcium sensing mechanisms. The free cytosolic concentration of Mg^{2+} in mammalian cells ranges from 0.5 to 2 mM, which typically exceeds the free $[Ca^{2+}]_i$ by a factor of 10^4-10^5. In addition, cells contain trace amounts (total concentration $\approx 10^{-6}$ M) of divalent transition metals including manganese (Mn^{2+}), iron (Fe^{2+}), cobalt (Co^{2+}), nickel (Ni^{2+}), copper (Cu^{2+}) and zinc (Zn^{2+}) that might compete with Ca^{2+} for the binding sites in the calcium sensors. The chemical properties of the transition metals, however, strongly contrast to those of the physiologically important spherical divalent cations Ca^{2+} and Mg^{2+}. They have preferred coordination geometries and the bonds they form may have a pronounced covalent character (Falke *et al.*, 1994). It is generally believed that a large fraction of the transition metals are statically bound to the structures and molecules in cells, contrasting to the dynamic role of calcium in many biological processes.

The structure and function of molecules that bind divalent cations have been extensively investigated *in vitro* with NMR and X-ray crystallography. The conditions present in these kinds of experiments are usually far from those in living cells, and therefore a correspondence between the results and physiological function is not always clear. Quantitative studies on the functional properties of calcium sensor proteins in their natural surroundings are much more scarce, largely due to the lack of proper model systems.

In this study we used the mouse rod photoreceptor cell as a physiological model system to investigate the functional properties of Ca^{2+} signaling proteins in their natural cellular environment. In rods phototransduction is modulated by changes in $[Ca^{2+}]_i$. Absorption of photons by the visual pigment molecules, rhodopsins, triggers a biochemical cascade that leads to an increased hydrolysis of cGMP by phosphodiesterase (PDE6) in the rod outer segment (ROS). The consequent decrease in [cGMP] closes the non-selective cGMP-gated (CNG) cation channels in the ROS plasma membrane, leading to a decreased inflow of Na^+ and Ca^{2+} into ROS (reviewed in Pugh, Jr. & Lamb, 2000). Since Ca^{2+} is continuously extruded from the cytoplasm by the Na^+/ Ca^{2+}, K^+ exchangers (NCKX1, Cervetto *et al.*, 1989), $[Ca^{2+}]_i$ declines in light. In mouse rods $[Ca^{2+}]_i$ is ~250 nM in darkness and drops to ~20 nM in bright light (Woodruff *et al.*, 2002; Woodruff *et al.*, 2007). This decrease in $[Ca^{2+}]_i$ serves as a negative feedback signal that is mediated by the neuronal calcium sensor (NCS) proteins recoverin (Dizhoor *et al.*, 1991) and guanylyl cyclase activating proteins (GCAP1 and GCAP2 in rods, Gorczyca *et al.*, 1994; Dizhoor *et al.*, 1995), leading to a faster deactivation of R* (Chen *et al.*, 2010a) and to accelerated synthesis of cGMP by guanylyl cyclases (GCs, Lolley & Racz, 1982; Dizhoor *et al.*, 1994). In darkness when $[Ca^{2+}]_i$ is high, the Ca^{2+} - bound recoverin is attached to rhodopsin kinase (RK) and prevents it from phosphorylating R*. The light-induced decline of $[Ca^{2+}]_i$ and the subsequent dissociation of Ca^{2+} from the recoverin's EFh binding sites releases RK to phosphorylate R*, causing partial inactivation of R* (Chen *et al.*, 1995; Klenchin *et al.*, 1995; Makino *et al.*, 2004; Ames *et al.*, 2006). The phosphorylated R* binds arrestin, which leads to complete inactivation of R* (Wilden *et al.*, 1986). On the other hand, the activity regulation of GC is achieved through GCAPs (Koch & Stryer, 1988; Dizhoor *et al.*, 1995): In darkness with high $[Ca^{2+}]_i$, three of the four EF –hand (EFh) binding sites of a GCAP molecule are occupied with Ca^{2+}, making it incapable to activate a GC molecule. At low $[Ca^{2+}]_i$ dissociation of Ca^{2+} ions from the EFh binding sites makes the GCAP molecule a GC activator.

We studied the selectivity and functional properties of the Ca^{2+} sensor proteins recoverin and GCAP by recording *ex vivo* ERG rod photoresponses from intact isolated mouse retinas. We used light stimulus protocols and ion substitutions that should dissect the roles and function of recoverin and GCAP, respectively. Our approach is critically based on the assumption that the intracellular concentration of the divalent ion under study is regulated by light in rod outer segments, i.e. that the ion can permeate the CNG channel, and that NCKX1 can effectively extrude the ion from the cell. In this study we focused on Co^{2+}, which is a transition metal ion of similar size

as Mg^{2+} but much smaller than Ca^{2+} (effective ionic radii: Co^{2+} 0.75 Å (high spin), 0.65 Å (low spin), Mg^{2+} 0.72 Å, and Ca^{2+} 1.00 Å, Shannon, 1976), and it is a widely used Ca^{2+} channel blocker. Co^{2+} is known to stabilize the structure of vitamin B_{12} and it forms an integral part of some metalloproteins (Kobayashi & Shimizu, 1999). Here we show that Co^{2+} can permeate the CNG channel and that, somewhat surprisingly, it also can be effectively extruded by NCKX1 from ROS. Our results also strongly suggest that Co^{2+} can mediate the negative feedback signals through both CGAP and recoverin very much like Ca^{2+} does.

2. Material and Methods

2.1 Ethical approval

The use and handling of the animals were in accordance with the Finland Animal Welfare Act 1986 and guidelines of the Animal Experimentation Committee of The University of Helsinki, Finland.

2.2 The ERG experiments

Pigmented mice (C57Bl/6) were dark-adapted overnight. The animals were sacrificed by CO_2 inhalation and decapitation, the eyes were enucleated and bisected along the equator, and the retinas were detached in cooled Ringer under dim red light. The isolated retina was placed in a specimen holder (Donner, Hemilä, & Koskelainen, 1988) with an active recording area of 1.2 mm. The upper (photoreceptor) side was superfused with a constant flow (*ca.* 1.5 ml/min) of Ringer's solution. Experiments were conducted at 25°C in a medium containing (mM): Na^+, 133.9; K^+, 3.3; Mg^{2+}, 2.0; Ca^{2+}, 1.0; Cl^-, 143.2; glucose, 10.0; EDTA, 0.01; HEPES, 12.0, buffered to pH 7.5 (at room temperature) with 5.8 mM NaOH. Sodium l-aspartate (2 mM) was added to block synaptic transmission to second-order neurons. Leibovitz culture medium L-15 (Sigma), 0.72 mg/ml, was added to improve the viability of the retina in all experiments. In addition, $BaCl_2$ (10 mM) was added in the lower electrode space, from where it would diffuse to the retina to suppress glial currents by blocking potassium channels located mainly at the endfeet of Müller cells (Bolnick, Walter, & Sillman, 1979; Nymark et al., 2005). The temperature was controlled by a heat exchanger below the specimen holder and monitored with a thermistor in the bath close to the retina.

2.3 Recording and light stimulation

The transretinal potential was recorded with two Ag/AgCl pellet electrodes, one in the subretinal space and the other in chloride solution connected to the perfusion Ringer through a porous plug. The DC signal was low-pass filtered (Bessel 8 pole with f_c = 300 – 1000 Hz) and sampled at 200–10000 Hz with a voltage resolution of 0.25 μV.

Light stimuli with homogeneous full-field illumination to the distal side of the retina were provided by a dual-beam optical system adapted from the setup used by Donner et al. (1988). In brief, 20 ms light flashes and/or longer light steps were generated with a 543.5 nm HeNe laser (Melles Griot 05 LGR 173, 0.8 mW) and a 633 nm HeNe laser (Melles Griot 25 LHR 151, 5 mW) and a Compur shutter for both laser paths, the midpoint of the flash indicating the zero time for the recordings. The Gaussian profile of the laser beam was flattened by conducting the beam through a light guide with mixing fibers. The uniformity of the beam at the level of the retina was confirmed with a small aperture photodiode. The light intensity of each source was controlled separately with calibrated neutral density filters and wedges.

The absolute intensity of the unattenuated laser beam (photons $mm^{-2}s^{-1}$) incident on the retina was measured in each experiment with a calibrated photodiode (EG&G HUV-1000B; calibration by the National Standards Laboratory of Finland). The amount of isomerizations (R*) produced by the stimulating flash light in individual rods was calculated as described in Heikkinen et al. (2008).

2.4 Chemicals and pharmacological manipulations

All chemicals were purchased from Sigma-Aldrich. The low $[Ca^{2+}]_{free}$ (25 nM) solutions were prepared using EGTA and the free $[Ca^{2+}]$ was calculated with an "EGTA calculator" (Portzehl, Caldwell, & Rueegg, 1964) taking into account 2 mM $[Mg^{2+}]$ present in our Ringer's solution. pH was adjusted to 7.5 with NaOH.

2.5 Analysis

2.5.1 Determination of rod's sensitivity to light flashes ($\Phi_{½}$)

Mixed exponential and Michaelis functions, operation curves, (Nymark *et al.*, 2005)

$$r_{\max} = r_{sat}\left(\alpha\left(1-e^{-\frac{\Phi}{\Phi_{½}}}\right)+(1-\alpha)\frac{\Phi}{\Phi+\Phi_{½}}\right) \quad (1)$$

were fitted to the measured flash response amplitude data to find the flash strength (Φ) that produce the half-maximal response ($\Phi_{½}$). r_{sat} is the amplitude of saturated rod response measured at plateau and α is the weighting factor between 0 and 1.

2.5.2 Determination of amplification constant (A)

The gain of phototransduction activation reactions was quantified by determining the amplification constant A (LP model, Lamb & Pugh, Jr., 1992) from the responses to short flashes. A delayed Gaussian function

$$r(t) = r_{sat}\left(1 - \exp[-\tfrac{1}{2}\Phi A(t - t_d)^2]\right) \quad (2)$$

was fitted to the leading edge of the measured ERG responses. There, r_{sat} is the saturated rod response amplitude (measured at the peak, see Fig. 1A and A1) and t_d combines the delays of phototransduction reactions and measurement electronics. The choice of maximal amplitude in ERG is somewhat arbitrary and the amplification constant determined here might not accurately describe the absolute value of the molecular amplification. However, this choice yields consistent results that can be also compared to A determined in low Ca^{2+} conditions. It should be noted, however, that the assumption regarding [cGMP] in ROS (< ~5 μM in the LP model) is not necessarily satisfied in very low [Ca^{2+}]. Thus, a model that does not assume low [cGMP] is presented in the Appendix to allow simulation of flash responses also during low Ca^{2+} exposures.

3. Results

3.1 Function of GCAP and recoverin in the intact retina can be probed with ex vivo ERG technique

We used the step/flash protocol (Fain *et al.*, 1989) to investigate the function of GCAP and recoverin, respectively, in mouse rods. Fig. 1A illustrates the ERG responses (fast PIII) of an isolated mouse retina to step/flash stimuli in conditions where the glial component and the components from the higher-order neurons had been pharmacologically removed (see Methods). In this protocol steps of light (I_{step} = 40 – 500 R^*s^{-1} per rod in Fig. 1A) were followed by a 20 ms bright light flash (Φ = 700 R^* per rod in Fig. 1A) presented simultaneously with the extinction of the light step. The characteristic features of the step-flash responses are the response recovery during the step and the shortening of the time spent in saturation after the flash as a function of the step intensity. It is worth to note that the experiments presented in this study were conducted under lowered temperature (25 °C) to increase the stability of the recordings leading to overall deceleration of photoresponse kinetics.

The roles of GCAP and recoverin can be dissected in the step/flash paradigm in the following way: The partial recovery of the light response (and thus the CNG channel current) during the response to steps of light is caused by the acceleration of both GC activity and rhodopsin deactivation (the role of calcium/calmodulin-mediated modulation of the cGMP channel conductance is thought to be of minor importance in mammalian rods). The recovery phase during a step at body temperatures consists of a fast (τ < 1 s) and a slow (τ ~ 100 s) exponential decay component, the fast of which is absent in GCAP1/GCAP2 knockout mice (Chen *et al.*, 2010b) but present in the recoverin knockout mice (Makino *et al.*, 2004), suggesting that the fast component of the recovery reflects the activation of GC by the GCAPs. Therefore, the occurrence of the fast component in step recovery can be used as an indication of functionality of the GCAP-mediated feedback. On the other hand, the deactivation kinetics of the flash response following the light step can be used as an indicator of the function of recoverin. The responses to flashes of constant strength begin their recovery progressively

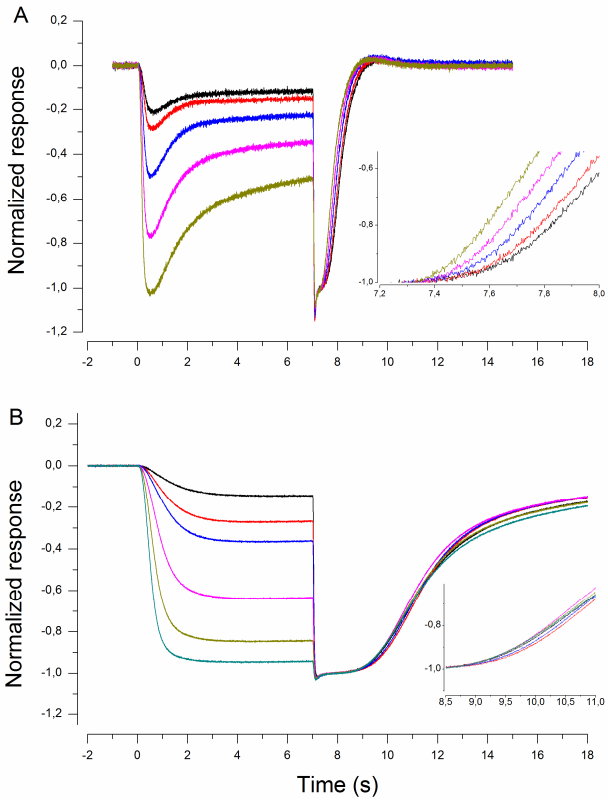

Figure 1 Step/flash protocol in physiological $[Ca^{2+}]_o$ (A) and 25 nM $[Ca^{2+}]_o$ (B). 7 s steps of light are followed by 20 ms flash at t = 7 s. Step intensities 40, 70, 130, 250 and 500 R^*s^{-1} in A, and 25, 40, 70, 130, 250 and 500 R^*s^{-1} per rod in B. Flash strength was 700 R* per rod in A and 7000 R* per rod in B.

faster when the step intensity is increased: this has been shown to reflect the shortening of R* lifetime (τ_R) in response to the lowered steady state level of $[Ca^{2+}]_i$ due to the step (Matthews, 1995; Fain *et al.*, 2001; Hamer *et al.*, 2005). Because the shortening of τ_R is mediated by recoverin (Chen *et al.*, 2010a), the reduction of the saturation time (T_{sat}) after the flash in the step/flash experiments can be used to probe the action of recoverin.

To verify that the Ca^{2+} dependent mechanisms are responsible for the response relaxation during step illumination and for the shortening of T_{sat} in the step/flash experiments we removed almost all Ca^{2+} from the perfusate. As is clearly evident in Fig. 1B, both the response recovery during the steps and the shortening of T_{sat} of the flash responses were completely removed when the retina was perfused with low (25 nM) free $[Ca^{2+}]_o$ solution. This low calcium state served as a reference state in which all the Ca^{2+} feedback mechanisms involved in the phototransduction are disabled.

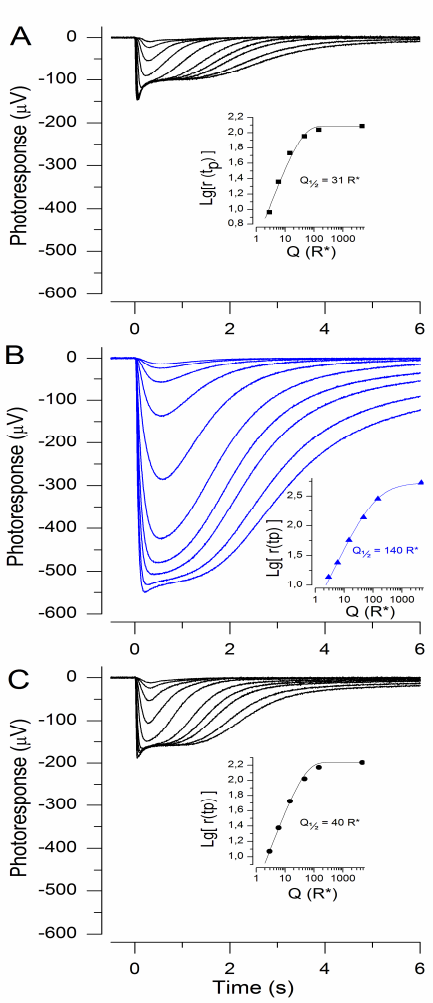

Figure 2 Saturated photoresponse amplitude increases and fractional sensitivity decreases reversibly in low 25 nM free [Ca^{2+}]. Photoresponse families to 20 ms light flashes recorded from the same mouse retina, A) in modified Ringer's with 1 mM [Ca^{2+}], B) in modified Ringer's with 25 nM free [Ca^{2+}] once a steady state has been reached, and C) in 1 mM Ca^{2+} after low Ca^{2+} exposure. Flash strengths were Q = 2.9, 5.9, 14.7, 46.6, 147.4, 466, 930, 1474, 2940 and 4660 R*. Insets show the response-intensity data. Operation curves fitted to data points (see Methods) yield $\Phi_{½}$ = 31, 140 and 40 R* in 1 mM Ca^{2+}, 25 nM Ca^{2+} and in 1 mM Ca^{2+} after low Ca^{2+} exposure.

3.2 Stable and large rod responses can be measured in 25 nM $[Ca^{2+}]_o$ with *ex vivo* ERG technique

The most elemental tool for assessing rod physiology is the dark-adapted cell's impulse response, in which the calcium-dependent feedback can also be readily observed. Fig. 2A shows fast PIII responses to 20 ms light flashes of increasing strength recorded from a dark-adapted isolated mouse retina in 1 mM $[Ca^{2+}]_{out}$. When Φ exceeded ~150 R*, the plateau level amplitude of

the responses did not further grow with increasing flash strength while T_{sat} remained growing, indicating that all the CNG channels are closed. The dependence of the response amplitude (r_{max}) on flash strength is shown in the inset of Fig. 2A. Here, the maximal saturated response amplitude was read at the plateau level after the transient peak component (the nose, Vinberg *et al.*, 2009). With this choice the flash strength that elicited the half-maximal response ($\Phi_{½}$) was 26 ± 2 R* (n = 13).

When the retina was exposed to low Ca^{2+} perfusion (~25 nM free $[Ca^{2+}]_{out,}$ Fig 2B), the saturated response amplitude grew first up to ~1000 μV (sometimes even larger) but decreased then to a steady state level that in this retina was still 5-fold (2.6 ± 0.4-fold, n = 10) larger compared to those recorded in 1 mM Ca^{2+}. The low-calcium perfusion also abolished the nose component consistently with our previous data (Vinberg *et al.*, 2009, Vinberg & Koskelainen, 2010). Moreover, the responses were very well restored close to their initial shape and size when returned to 1 mM $[Ca^{2+}]_{out}$ after ca. 90 minutes exposure to low calcium (Fig. 2C). Thus mouse rods can maintain stable and relatively large responses in the very low 25 nM $[Ca^{2+}]_{out}$ and even long exposures to low calcium do not bring about irreversible changes in the state of the rods .

The increased amplitude of the saturated responses in low Ca^{2+} is consistent with the current model of phototransduction that Ca^{2+} inhibits GC through binding to GCAP. Removal of most of the Ca^{2+} relieves this inhibition, leading to an increased [cGMP] in the rod outer segment (ROS) and consequent increase in the CNG channel current. Instead, decrease of a rod fractional sensitivity, demonstrated as an increased $\Phi_{½}$ during low Ca^{2+} exposure (inset of Fig. 2B), is harder to reconcile with the current picture of phototransduction. However, it will be demonstrated in Discussion that the high [cGMP] during low Ca^{2+} perfusion can indeed account for the decreased gain of phototransduction activation reactions, and this could explain the desensitization of rods in 25 nM $[Ca^{2+}]_o$.

3.3 Co^{2+} can prevent acceleration of GC activity by GCAP

The ability of Co^{2+} to control cGMP synthesis was first investigated by comparing the impulse responses of dark-adapted rods in the presence of 1 mM $[Ca^{2+}]_o$ and in 1 mM $[Co^{2+}]_o$ without any Ca^{2+}. Fig. 3 shows responses from one retina to similar sets of 20 ms light flashes first in 1 mM $[Ca^{2+}]_o$ (A) and then in 1 mM $[Co^{2+}]_o$ (B). The shape and size of the responses to

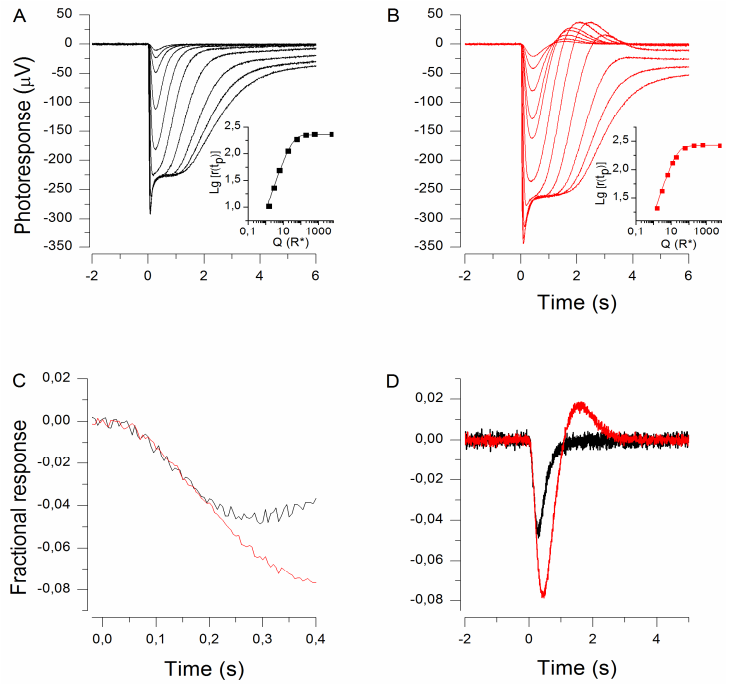

Figure 3 *Rod impulse responses in 1 mM $[Ca^{2+}]_{out}$ (A) and when Ca^{2+} has been replaced by 1 mM $[Co^{2+}]_{out}$ (B).* Photoresponse families to 20 ms light flashes producing 2 – 6400 R*rod^{-1} (A and B). Insets plots the logarithm of response amplitude R as a function of Q. Mixed exponential and Michaelis functions have been fitted to data points yielding $Q_{½}$ = 30 and 19 R*rod^{-1} in 1 mM Ca^{2+} and in 1 mM Co^{2+}, respectively. (C) Smallest responses from A (black) and B (red, Q = 1.6 R*rod^{-1}) shown in short time scale. Responses have been normalized by R_{sat}. (D) Same responses as in C shown in extended time scale.

corresponding stimuli were remarkably similar when compared to those recorded in low calcium (Fig. 2B): The saturated response amplitude grew only slightly from about 230 µV to 270 µV (read at the plateau level), indicating that guanylate cyclase activity was not changed much when Ca^{2+} was replaced with Co^{2+}. Further, the nose component remained practically unaffected, while in the recovery phase a pronounced overshoot was evident in all responses in the cobalt solution. The flash strength needed to elicit a half-maximal response decreased from 30 R* in 1 mM $[Ca^{2+}]_o$ to 19 R* in 1 mM $[Co^{2+}]_o$. Fig. 3C compares the rising phase kinetics of the responses to the dimmest flash (Q = 1.6 R*) from panels A and B. The initial rising phases of the responses recorded in the Ca^{2+} and Co^{2+} solutions coincide closely, but the response shut-off is somewhat slower in Co^{2+} than in Ca^{2+} solution. Fig. 3D shows the responses of panel C on an extended time scale. It clearly shows the delayed shut-off in Co^{2+} and an overshoot at the end of the response.

Similar results were obtained in all corresponding experiments from seven retinas. The average saturated response amplitude was 140 ± 20 µV

in Ca^{2+} solution and grew to 180 ± 30 μV (n = 7) as Co^{2+} was substituted for Ca^{2+}. The large transient increase in saturated response amplitudes observed in low Ca^{2+} was never seen when Ca^{2+} was replaced with Co^{2+}. Instead, always when 1 mM Co^{2+} was introduced under low calcium perfusion, the photoresponse sizes were restored from the "typical huge low calcium" responses to the "typical normal-size cobalt" responses and the slow initial rising phases of the responses recorded in low calcium were restored to similar observed in 1 mM Ca^{2+} (and Co^{2+}) . The $\Phi_{½}$ decreased from 24 ± 3 R* in 1 mM $[Ca^{2+}]_o$ to 17 ± 1 R*in 1 mM $[Co^{2+}]_o$ (n = 7). The identical initial rising phases of the responses in 1 mM Ca^{2+} and 1 mM Co^{2+} indicate that the amplification factor of mouse rod phototransduction is not affected by the replacement of Ca^{2+} with Co^{2+}. Thus Co^{2+} can prevent (1) the large increase of saturated response amplitude, (2) the deceleration of activation reactions, and (3) the decrease in fractional sensitivity (i.e. increased $\Phi_{½}$) that were all caused by the absence of Ca^{2+} (see above). This suggests that Co^{2+} can inhibit GC in a similar way as Ca^{2+} does, and thus prevent the excessive increase of [cGMP] in ROS upon removal of Ca^{2+} from the perfusion.

3.4 Co^{2+} can replace Ca^{2+} in the dynamic modulation of GC activity and R* lifetime during light response

Figures 4A and B illustrate a similar step/flash experiment as in Fig. 1, recorded from another retina. Similarly to Fig. 1A, the recovery phases during the steps of light as well as the acceleration of the flash response recovery with increasing step intensity were present under 1 mM $[Ca^{2+}]_o$ (panel A), indicating that the Ca^{2+}-dependent modulations of both GC activity and τ_R were functional. Once again these modulations disappeared under 25 nM $[Ca^{2+}]_o$ (panel B). The retina was next exposed to a solution with all Ca^{2+} replaced with an equimolar concentration of Co^{2+} (panel C). A similar recovery during the step illuminations as with Ca^{2+} was present, indicating that Co^{2+} can mediate the dynamic modulation of GC activity. Also, the acceleration of the flash response recovery with increasing step intensity that was absent under low calcium was restored by Co^{2+}. This strongly suggests that τ_R is shortened by a light-induced decrease of $[Co^{2+}]_i$ in the rod outer segment.

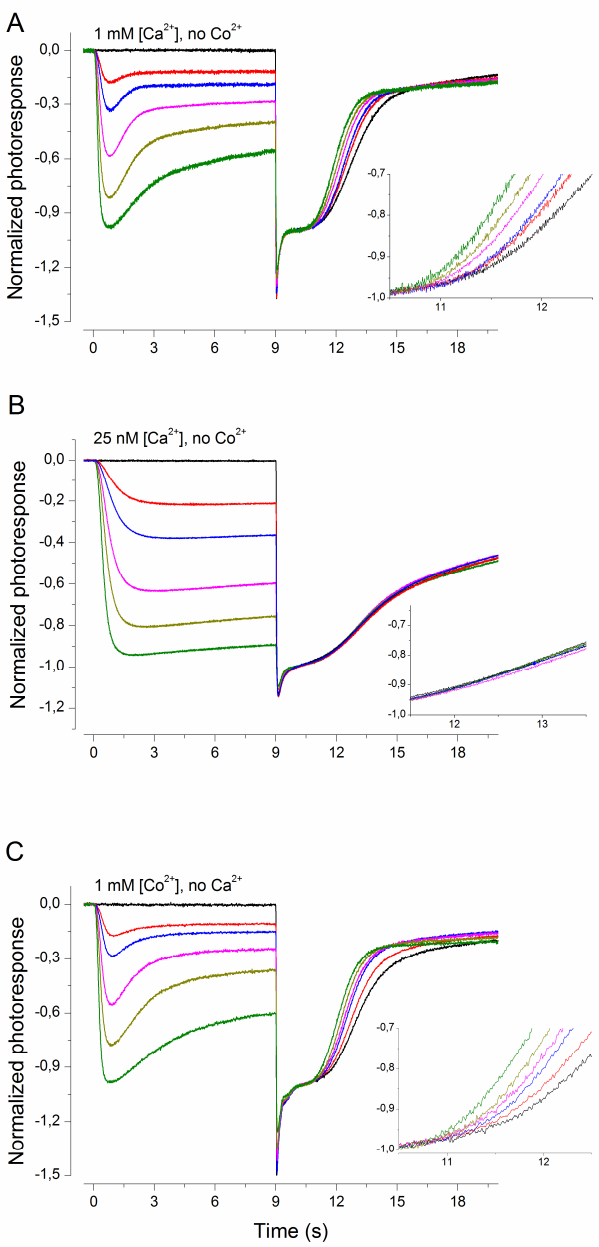

Figure 4 *Step/flash protocol in 1 mM [Ca²⁺]₀ (A), in 25 nM [Ca²⁺]₀ (B) and in 1 mM [Co²⁺]₀ without Ca²⁺ (C).* 9 s steps of light (I_{step} = 0, 10, 20, 40, 80, 160 R*s⁻¹rod⁻¹) are followed by a 20 ms flash (Q = 6400 R* rod⁻¹) at t = 9 s.

4. Discussion

4.1 Studying the functionality of mouse recoverin and GCAPs by ex vivo ERG

The phototransduction machinery of the vertebrate rod photoreceptor can act as a unique model system allowing quantitative investigations on the function of several proteins involved in G-protein or calcium-mediated signaling. Here we focused our study on the functional and selectivity properties of two NCS proteins belonging to the large EF-hand superfamily, namely GCAP and recoverin that are both expressed in mouse rod photoreceptors. The function of these proteins has been investigated with experimental protocols using the suction pipette technique, and their physiological importance in mediating Ca^{2+} signals in mouse rods has been clearly established (Mendez *et al.*, 2001; Makino *et al.*, 2004; Chen *et al.*, 2010a).

Since the EF hands of both recoverin and GCAPs are highly selective for Ca^{2+} over Mg^{2+} and possibly over other divalent cations, it is important that the ionic compositions are not different around the different parts of the cell(s) under study. In the suction pipette approach the outer segment of mouse rod is usually sucked into the pipette, making it difficult to simultaneously switch between different perfusates around the outer and the inner segment. To circumvent this problem we used the step/flash protocol in the *ex vivo* ERG on isolated mouse retinas. To our knowledge this was the first time this protocol was applied in *ex vivo* ERG. Our data clearly shows that the dynamic modulations of both GC activity and R* lifetime can be reliably investigated by the step/flash protocol from an intact mouse retina with this technique. Further, it can be used to study the divalent ion specificity of the GCAP- and recoverin mediated feedback mechanisms whenever the intracellular concentration of the divalent ion under study is dynamically controlled by light, i.e. when it can permeate the CNG channel and it is extruded by the NCKX.

4.2 Low $[Ca^{2+}]_o$ can provide a stable state in which the GCAP- and recoverin-mediated feedback signals are disabled

To test whether other divalent cations besides Ca^{2+} can modulate GC activity and τ_R, it was important to find stable conditions where $[Ca^{2+}]_i$ is below the operating ranges controlling the activities of GCAP and recoverin. We found that a stable state with large and recurrent responses could be achieved in an EGTA buffered medium with free extracellular $[Ca^{2+}]$ below ~10^{-7} M (Fig. 1B). It is reasonable to assume that even in these conditions the NCKX1s were able to keep the intracellular $[Ca^{2+}]$ lower than the extracellular $[Ca^{2+}]$. If so, the intracellular calcium concentration at 25 nM $[Ca^{2+}]_o$ would always be below that in bright light under normal $[Ca^{2+}]_o$, suggesting that the modulations of both GC activity and R* lifetime should be absent. This was clearly supported by our data (Figs. 2B and 4B).

The rod impulse responses show, however, changes in several distinct features when exposed to low calcium conditions. When switched to 25 nM $[Ca^{2+}]_o$, the saturated photoresponse amplitude first grows several fold and then returns in minutes to a steady state still more than twice as large as in normal calcium. At the same time the photoresponse kinetics is decelerated, the rods' sensitivity to flashes of light is strongly decreased, and the amplification constant determined from the leading edges of the responses is lower compared to that in normal calcium. We felt using the 25 nM $[Ca^{2+}]_o$ condition as a reliable reference state required clarification of the mechanisms leading to the seemingly unphysiological properties of the photoresponses under low Ca^{2+} (see below).

4.3 Elevated cGMP can explain most of the changes in photoresponses induced by low $[Ca^{2+}]_o$

Lowering external calcium has three known effects on the phototransduction machinery: The rate of rhodopsin deactivation is increased through removal of calcium-controlled inhibition of rhodopsin kinase by recoverin, the guanylate cyclase activity is increased by removal of the calcium-dependent inhibition of GCAP, and the single CNG channel conductance (g_{cG}) is increased by removing the Ca^{2+}-induced partial block of the channel (Haynes *et al.*, 1986). The acceleration of rhodopsin deactivation clearly cannot explain the major changes in response amplitude and kinetics, but the raised [cGMP] due to the acceleration of GC activity and the increased g_{cG} together lead to a very large CNG channel current (J_{cG}) in low Ca^{2+} conditions. The initial large increase of saturated response amplitudes, followed by a decrease to a steady state, suggests that the physiological ion gradients cannot be maintained under low Ca^{2+} exposure, i.e. initially after switching to low Ca^{2+} perfusion J_{cG} is highly

boosted due to the accelerated GC activity and increased g_{cG} but becomes gradually constrained by decreased ion gradients. However, differently from single cell recordings with suction electrodes on toad rods in very low $[Ca^{2+}]_o$ (Yau *et al.*, 1981), a steady state with relatively large saturated response amplitude (reflecting high J_{cG}) could be achieved in our *ex vivo* ERG experiments on intact mouse retinas (see Fig. 2B).

Our observation that the sensitivity of mouse rods to light flashes is decreased and response kinetics is decelerated under very low $[Ca^{2+}]_o$ is consistent with the results from isolated amphibian rods (Hodgkin *et al.*, 1984; Matthews, 1995). It has been suggested that the desensitization of rods and the instability of the responses in very low $[Ca^{2+}]_o$ in suction pipette recordings might be due to accumulation of Na^+ into ROS and/or high metabolic stress caused by the very large J_{cG} (Yau *et al.*, 1981; Matthews, 1995; Hodgkin *et al.*, 1984). In a previous work (Vinberg & Koskelainen, 2010: their Fig. 7) we demonstrated that accumulated Na^+ or large metabolic load are not likely to explain the reduced sensitivity and decelerated response kinetics of rods during low Ca^{2+} exposure. Instead, Matthews has suggested that increased [cGMP] can explain at least some of the effects caused by very low Ca^{2+} (Matthews, 1995). We investigated this by modeling as a potential explanation for the compromised efficiency of the phototransduction activation reactions in the rod impulse responses in low $[Ca^{2+}]_o$. The overall amplification constant A defined by the LP model (Lamb & Pugh, Jr., 1992) decreased from 2.6 ± 0.3 s^{-2} in physiological medium to 0.4 ± 0.1 s^{-2} under low Ca^{2+} conditions (n = 4). However, the LP model assumes that [cGMP] is below ~5 μM, a condition that is not likely satisfied in very low $[Ca^{2+}]$. We thus implemented a model, largely based on the equations reviewed in Pugh et al. (Pugh *et al.*, 2000), that does not pose requirements on [cGMP] in ROS and thus can be used also under low Ca^{2+} conditions (see Appendix). Simulations of dim flash responses with this model was used to predict the steady state [cGMP] (*i.e.* [cGMP] preceding the flash, cG_{dark}) that in normal external calcium concentration is about 4 μM (reviewed in Pugh & Lamb, 1990). Fitting the simulated responses to the measured responses in low Ca^{2+} gave [cGMP] values between 10 and 40 μM (see Fig. A1 in the Appendix), consistent with previous biochemical and electrophysiological data regarding the acceleration of GC activity in low Ca^{2+} (Koch & Stryer, 1988; Koutalos *et al.*, 1995; Mendez *et al.*, 2001). The values obtained, however, were very sensitive to the choice of half-activation concentration of [cGMP] for PDE (K_m, see Eq. in Appendix). The most recent estimate for K_m is 10 μM (Leskov *et al.*, 2000), which yielded cG_{dark} = 17 ± 3 μM (n = 4). Previous

estimates for K_m were around 100 μM (reviewed in Pugh, Jr. & Lamb, 2000), and K_m yielded cG_{dark} = 28 ± 4 μM (n = 4). Despite the uncertainty regarding to the absolute value of cG_{dark} under low Ca^{2+} conditions, it is clear that the increase in cG_{dark} alone can explain the apparent decrease of A and the deceleration of the photoresponse kinetics in low Ca^{2+}. Additional evidence for the role of large cG_{dark} in low Ca^{2+} was achieved experimentally by decreasing [cGMP] during low Ca^{2+} exposure with background illumination. Indeed, both A and fractional sensitivity were increased by application of background light, indicating that large [cGMP] really can decelerate activation kinetics and reduce sensitivity under low Ca^{2+} conditions (data not shown). These simulations and experimental data together suggest that high cG_{dark} alone is able to account for the decelerated activation kinetics and decreased fractional sensitivity during low Ca^{2+} treatments, and that the low $[Ca^{2+}]_o$ (25 nM) exposure drives the rods (at least when embedded in the intact isolated retina as in the *ex vivo* ERG) into a stable state that can serve as a reference state with all the known calcium-dependent feedback mechanisms of phototransduction disabled.

4.4 Co^{2+} can mediate modulation of GC activity and R* lifetime in rod photoreceptors

As discussed above, removal of most of the Ca^{2+} from the perfusion led to a steady state in which [cGMP] of the ROS is larger than in physiological conditions, giving rise to (1) increased saturated response amplitude, (2) decelerated activation kinetics, and (3) lowered fractional sensitivity of rod phototransduction (see Fig. 2). Introduction of Co^{2+} canceled all these effects (see Fig. 3), suggesting that 1 mM $[Co^{2+}]_o$ was able to inhibit GC inside the ROS and thereby return the intracellular cGMP level close that in the presence of 1 mM $[Ca^{2+}]_o$. These results strongly suggest that Co^{2+} can permeate the CNG channel, bind to GCAP, and prevent it from activating GC. Moreover, the step/flash experiments showed that the dynamic modulations of both GC activity and τ_R during light response can be accomplished with Co^{2+} instead of Ca^{2+} as the signaling ion and that the kinetics of these modulations is quite similar in the presence of Co^{2+} compared to those with Ca^{2+}. This inevitably requires that $[Co^{2+}]_i$ is regulated very much in the same way as Ca^{2+}. Thus, we suggest that Co^{2+} can be extruded by NCKX and it seems likely that Co^{2+} can bind to and dissociate from both GCAP and recoverin much like Ca^{2+} does. These results also suggest that the bindings and dissociations of Co^{2+} bring about corformational changes of the same kind as produced by Ca^{2+} and that the proteins can perform the same molecular functionalities in the presence of Ca^{2+}.

4.5 About the selectivity mechanisms of EF-hand proteins

In this study we concluded that the EF-hand binding sites of GCAP and recoverin are not selective against Co^{2+}. This is somewhat surprising since the EF-hand binding pocket is very specific against Mg^{2+} (for review see Gifford *et al.*, 2007). The selectivity mechanism is thought to be based on the smaller ionic radius of Mg^{2+} compared to that of Ca^{2+} and on the consequent preference for a distinct coordination geometry (Gifford *et al.*, 2007). This explanation sounds natural since Mg^{2+} and Ca^{2+} are chemically very similar and the only significant difference between them is the physical size. However, the ionic radii of Co^{2+} and Mg^{2+} are of the same size. Thus, it seems that the selectivity mechanisms of the EFh binding sites are complicated and also other properties than the ionic radius determine their specificity against various divalent cations. Interestingly, several types of voltage-gated Ca^{2+} channels *are* selective and can discriminate between Ca^{2+} and Co^{2+}, the latter of which actually is a widely used calcium channel blocker at concentrations used in this study. Our results suggest that the EF-hands of NCS proteins may be engineered to discriminate effectively only between Ca^{2+} and Mg^{2+}, the latter of which is abundantly present in cells, but they might not be specific against other divalent cations present as trace elements in physiological systems.

Reference List

Ames JB, Levay K, Wingard JN, Lusin JD, & Slepak VZ (2006). Structural basis for calcium-induced inhibition of rhodopsin kinase by recoverin. *J Biol Chem* **281**, 37237-37245.

Cervetto L, Lagnado L, Perry RJ, Robinson DW, & McNaughton PA (1989). Extrusion of calcium from rod outer segments is driven by both sodium and potassium gradients. *Nature* **337**, 740-743.

Chen CK, Inglese J, Lefkowitz RJ, & Hurley JB (1995). Ca(2+)-dependent interaction of recoverin with rhodopsin kinase. *Journal of Biological Chemistry* **270**, 18060-18066.

Chen CK, Woodruff ML, Chen FS, Chen D, & Fain GL (2010a). Background light produces a recoverin-dependent modulation of activated-rhodopsin lifetime in mouse rods. *J Neurosci* **30**, 1213-1220.

Chen J, Woodruff ML, Wang T, Concepcion FA, Tranchina D, & Fain GL (2010b). Channel modulation and the mechanism of light adaptation in mouse rods. *J Neurosci* **30**, 16232-16240.

Dizhoor AM, Lowe DG, Olshevskaya EV, Laura RP, & Hurley JB (1994). The human photoreceptor membrane guanylyl cyclase, RetGC, is present in outer segments and is regulated by calcium and a soluble activator. *Neuron* **12**, 1345-1352.

Dizhoor AM, Olshevskaya EV, Henzel WJ, Wong SC, Stults JT, Ankoudinova I, & Hurley JB (1995). Cloning, sequencing, and expression of a 24-kDa Ca(2+)-binding protein activating photoreceptor guanylyl cyclase. *Journal of Biological Chemistry* **270**, 25200-25206.

Dizhoor AM, Ray S, Kumar S, Niemi G, Spencer M, Brolley D, Walsh KA, Philipov PP, Hurley JB, & Stryer L (1991). Recoverin: a calcium sensitive activator of retinal rod guanylate cyclase. *Science* **251**, 915-918.

Fain GL, Lamb TD, Matthews HR, & Murphy RL (1989). Cytoplasmic calcium as the messenger for light adaptation in salamander rods. *Journal of Physiology* **416**, 215-243.

Fain GL, Matthews HR, Cornwall MC, & Koutalos Y (2001). Adaptation in vertebrate photoreceptors. [Review] [299 refs]. *Physiological Reviews* **81**, 117-151.

Falke JJ, Drake SK, Hazard AL, & Peersen OB (1994). Molecular tuning of ion binding to calcium signaling proteins. *Q Rev Biophys* **27**, 219-290.

Gifford JL, Walsh MP, & Vogel HJ (2007). Structures and metal-ion-binding properties of the Ca2+-binding helix-loop-helix EF-hand motifs. *Biochem J* **405**, 199-221.

Gorczyca WA, Gray-Keller MP, Detwiler PB, & Palczewski K (1994). Purification and physiological evaluation of a guanylate cyclase activating protein from retinal rods. *Proceedings of the National Academy of Sciences of the United States of America* **91**, 4014-4018.

Hamer RD, Nicholas SC, Tranchina D, Lamb TD, & Jarvinen JL (2005). Toward a unified model of vertebrate rod phototransduction. *Visual Neuroscience* **22**, 417-436.

Haynes LW, Kay AR, & Yau KW (1986). Single cyclic GMP-activated channel activity in excised patches of rod outer segment membrane. *Nature* **321**, 66-70.

Hodgkin AL, McNaughton PA, Nunn BJ, & Yau KW (1984). Effect of ions on retinal rods from Bufo marinus. *Journal of Physiology* **350**, 649-680.

Klenchin VA, Calvert PD, & Bownds MD (1995). Inhibition of rhodopsin kinase by recoverin. Further evidence for a negative feedback system in phototransduction. *Journal of Biological Chemistry* **270**, 16147-16152.

Kobayashi M & Shimizu S (1999). Cobalt proteins. *Eur J Biochem* **261**, 1-9.

Koch KW & Stryer L (1988). Highly cooperative feedback control of retinal rod guanylate cyclase by calcium ions. *Nature* **334**, 64-66.

Koutalos Y, Nakatani K, Tamura T, & Yau KW (1995). Characterization of guanylate cyclase activity in single retinal rod outer segments. *Journal of General Physiology* **106**, 863-890.

Lamb TD & Pugh EN, Jr. (1992). A quantitative account of the activation steps involved in phototransduction in amphibian photoreceptors. *Journal of Physiology* **449**, 719-758.

Leskov IB, Klenchin VA, Handy JW, Whitlock GG, Govardovskii VI, Bownds MD, Lamb TD, Pugh EN Jr, Arshavsky VY. (2000). The gain of rod phototransduction: reconciliation of biochemical and electrophysiological measurements. *Neuron* **27***,* 525-37

Lolley RN & Racz E (1982). Calcium modulation of cyclic GMP synthesis in rat visual cells. *Vision Research* **22**, 1481-1486.

Makino CL, Dodd RL, Chen J, Burns ME, Roca A, Simon MI, & Baylor DA (2004). Recoverin regulates light-dependent phosphodiesterase activity in retinal rods. *Journal of General Physiology* **123**, 729-741.

Matthews HR (1995). Effects of lowered cytoplasmic calcium concentration and light on the responses of salamander rod photoreceptors. *Journal of Physiology* **484**, 267-286.

Mendez A, Burns ME, Sokal I, Dizhoor AM, Baehr W, Palczewski K, Baylor DA, & Chen J (2001). Role of guanylate cyclase-activating proteins (GCAPs) in setting the flash sensitivity of rod photoreceptors. *Proceedings of the National Academy of Sciences of the United States of America* **98**, 9948-9953.

Nikonov S, Engheta N, Pugh EN, Jr., & Pugh EN (1998). Kinetics of recovery of the dark-adapted salamander rod photoresponse. *Journal of General Physiology* **111**, 7-37.

Nikonov S, Lamb TD, & Pugh ENJ (2000). The role of steady phosphodiesterase activity in the kinetics and sensitivity of the light-adapted salamander rod photoresponse. *Journal of General Physiology* **116**, 795-824.

Nymark S, Heikkinen H, Haldin C, Donner K, & Koskelainen A (2005). Light responses and light adaptation in rat retinal rods at different temperatures. *Journal of Physiology* **567**, 923-938.

Pepperberg DR, Cornwall MC, Kahlert M, Hofmann KP, Jin J, Jones GJ, & Ripps H (1992). Light-dependent delay in the falling phase of the retinal rod photoresponse. *Visual Neuroscience* **8**, 9-18.

Pugh EN, Jr. & Lamb TD. (1990). Cyclic GMP and calcium: the internal messengers of excitation and adaptation in vertebrate photoreceptors. *Vision Research* **30**, 1923-1948.

Pugh EN, Jr. & Lamb TD. Phototransduction in vertebrate rods and cones: molecular mechanisms of amplification, recovery and light adaptation. In "Molecular Mechanisms in Visual Transduction". Stavenga, D. G., DeGrip, W. J., and Pugh, E. N. Jr. First ed.[3], 183-255. 2000. Amsterdam, Elsevier. Handbook of Biological Physics. Hoff, A. J.
Ref Type: Serial (Book,Monograph)

Shannon RD (1976). Revised effective ionic radii and systematic studies of interatomic distances in halides and chalcogenides. *Acta Crystallographica Section A* **32**, 751-767.

Vinberg F & Koskelainen A (2010). Calcium sets the physiological value of the dominant time constant of saturated mouse rod photoresponse recovery. *PLoS ONE* **5**, e13025.

Vinberg FJ, Strandman S, & Koskelainen A (2009). Origin of the fast negative ERG component from isolated aspartate-treated mouse retina. *J Vis* **9**, 9-17.

Wilden U, Hall SW, & Kuhn H (1986). Phosphodiesterase activation by photoexcited rhodopsin is quenched when rhodopsin is phosphorylated and binds the intrinsic 48-kDa protein of rod outer segments. *Proceedings of the National Academy of Sciences of the United States of America* **83**, 1174-1178.

Woodruff ML, Olshevskaya EV, Savchenko AB, Peshenko IV, Barrett R, Bush RA, Sieving PA, Fain GL, & Dizhoor AM (2007). Constitutive excitation by Gly90Asp rhodopsin rescues rods from degeneration caused by elevated production of cGMP in the dark. *J Neurosci* **27**, 8805-8815.

Woodruff ML, Sampath AP, Matthews HR, Krasnoperova NV, Lem J, & Fain GL (2002). Measurement of cytoplasmic calcium concentration in the rods of wild-type and transducin knock-out mice. *Journal of Physiology* **542**, 843-854.

Yau KW, McNaughton PA, & Hodgkin AL (1981). Effect of ions on the light-sensitive current in retinal rods. *Nature* **292**, 502-505.

5. Appendix

5.1 Model for flash responses in very low [Ca^{2+}]

Here the equations that were used to simulate dim flash responses of rods under conditions where [Ca^{2+}] is below the operating range of Ca^{2+} feedback mechanisms are presented. They are used to simulate rod fast PIII responses to dim flashes in very low 25 nM free $[Ca^{2+}]_{out}$. The model is largely based on previously published equations (reviewed in Pugh *et al.*, 2000). The only difference is that here the approximations that require [cGMP] to be sufficiently small are omitted. This model ignores the possible shaping of the fast PIII responses by voltage-dependent ionic currents in the rod inner segment. The contribution of the inner segment currents on dim flash responses is, however, expected to be rather small since dim flashes cause changes of only few millivolts in the rod membrane potential. Moreover, they do not affect the initial activation phase of rod fast PIII responses (Vinberg *et al.*, 2009).

The CNG channel current (J_{cG}) can be expressed as function of [cGMP] (= cG) in ROS by the Hill equation

$$J_{cG} = J_{\max} \frac{cG^{n_{cG}}}{cG^{n_{cG}} + K_{cG}^{n_{cG}}}, \tag{3}$$

where J_{max} is the maximal CNG channel current with all channels open, K_{cG} is the half-activation concentration of cGMP (≈ 20 μM) and n_{cG} is the Hill coefficient (= 2 – 3). Since we simulated responses of dark-adapted rods to flashes of light, it is convenient to normalize J_{cG} to its value in darkness (= J_{dark}):

$$1 - \frac{J_{cG}}{J_{dark}} = R(t) = 1 - \frac{cG^{n_{cG}} \left(cG^{n_{cG}} + K_{cG}^{n_{cG}} \right)^{-1}}{cG_{dark}^{n_{cG}} \left(cG_{dark}^{n_{cG}} + K_{cG}^{n_{cG}} \right)^{-1}} \tag{4}$$

There, R(t) describes a rod response that is normalized with the maximal saturated response amplitude and cG_{dark} is the initial value of [cGMP] in darkness before presentation of a light flash.

We express the rate equation for cG as

$$\frac{dcG}{dt} = \alpha - \beta(t) K_m \frac{cG}{cG + K_m}, \quad (5)$$

where α is the rate of cGMP synthesis by GCs (in s^{-1}) and K_m is the Michaelis constant of hydrolysis reaction of cGMP by PDE. Note that since we use the model under conditions where α is not modulated by light, it can be assumed to be constant. Also it should be noted that this expression converges to the normally used expression for dcG/dt (= α - β *cG(t)*) when *cG* is much smaller than K_m. β includes the hydrolytic activity of all PDE molecules in darkness (β_{dark}, in s^{-1}) and the hydrolysis by light-activated PDE molecules (E*s)

$$\beta(t) = \beta_{dark} + E^*(t)\beta_{sub}, \quad (6)$$

where E*(t) describes the amount of activated PDE molecules as a function of time. β_{sub} is the hydrolysis rate of a single activated PDE subunit and can be expressed as (Lamb and Pugh, 1992)

$$\beta_{sub} = \frac{½ k_{cat} / K_m}{V_{cyto} N_{Av} B_{cG}}, \quad (7)$$

where V_{cyto} is the volume of the rod outer segment, N_{Av} is Avogadro's number and B_{cG} is the buffering power of the ROS for cGMP. However, this expression is not needed in our simulations since β_{sub} is embedded in the definition of the amplification constant (A) that can be determined from the flash responses under physiological [Ca^{2+}] (see 2.5.2).

The amount of activated PDE subunits due to short light flash producing Φ R*s can be described as (Nikonov *et al.*, 1998)

$$E^*(t) = \left\{ \Phi \exp\left[-\frac{t}{\tau_{ND}} \right] \right\} * \left\{ \nu_E \exp\left[-\frac{t}{\tau_D} \right] \right\}, \quad (8)$$

where ν_E is the rate at which single R* activates PDEs and "∗" denotes the convolution operator. The longer time constant is τ_D which in the mouse rod is thought to represent the lifetime time of PDE* (= τ_E). It can be determined from saturated rod flash responses by the "Pepperberg analysis" (Pepperberg *et al.*, 1992; Vinberg & Koskelainen, 2010). The shorter time constant (τ_{ND}) is then the lifetime of R* (= τ_R). In very low calcium conditions the synthesis rate of cGMP is high and constant, because it cannot be modulated during light responses. It can be calculated from the initial state by setting $dcG/dt|_{t=0} = 0$.

$$\alpha = \beta_{dark} K_m \frac{cG_{dark}}{cG_{dark} + K_m}. \quad (9)$$

Combining Eqs. (5), (6), (8) and (9) yields

$$\frac{dcG}{dt} = \beta_{dark} K_m \frac{cG_{dark}}{cG_{dark} + K_m} - K_m \left(\beta_{dark} + \Phi \frac{A}{n_{cG}} \right) \times \\ \times \left\{ \exp\left[-\frac{t}{\tau_{ND}} \right] \right\} * \left\{ \exp\left[-\frac{t}{\tau_D} \right] \right\} \quad , \qquad (10)$$

where the molecular description of the amplification constant $A = \nu_E \beta_{sub} n_{cG}$ under physiological conditions (Lamb & Pugh, Jr., 1992) has been used.

5.2 Simulations

The model presented above was used to simulate R(t) (Eq. (4)) to compare it with the fractional responses obtained from the *ex vivo* ERG recordings. The simulations were implemented into Matlab©, where R(t)s were calculated numerically.

In practice, first an initial guess for cG_{dark} was set and then $cG(t)$ was calculated point by point with Eq. (10), which then allowed the determination of R(t) with Eq. (4). In Eq. (10) estimates for n_{cG}, τ_R, τ_E, were needed. It was assumed that ν_E and β_{sub} are not affected by removal of Ca^{2+}. Thus, we used the LP model in normal Ca^{2+} to determine A (see 2.5.2) and set $n_{cG} = 3$. τ_E was determined with the Pepperberg analysis as earlier (Vinberg & Koskelainen, 2010). The choice of β_{dark} affected the deactivation kinetics, and it was chosen to match the initial recovery of experimentally measured R(t). τ_R was not critical in determining the recovery kinetics, since it was assumed to be the non-dominant time constant. It was set to be constant, 70 ms, in all simulations. Although the model could describe the full time course of flash response, here it was used to determine the initial value of [cGMP] (cG_{dark}) that best explained the decelerated initial activation kinetics in low Ca^{2+}. This analysis is not dependent on the choice of deactivation parameters (τ_R, τ_E and β_{dark}) since they do not affect the early activation kinetics of flash responses.

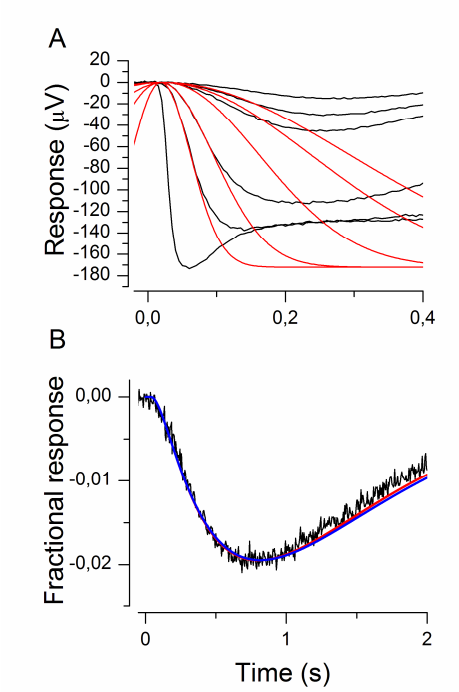

Figure A1 Determination of A with activation-only model (Lamb & Pugh, Jr., 1992) under physiological medium (A) and simulation of dim flash response under low 25 nM $[Ca^{2+}]_o$ (B). (A) A photoresponse family to 20 ms flashes at t = 0 s recorded in 1 mM $[Ca^{2+}]_o$ (black traces). Flash strengths Φ = 4.6, 7.3, 18.4, 58, 184 and 5800 R*s. Red traces plot the function r(t) (Eq. (2)) with A = 2.9 s^{-2}, t_d = 20 ms and r_{sat} = 172 μV. (B) A small-stimulus flash response under 25 nM $[Ca^{2+}]_o$ normalized with maximal saturated response amplitude at those conditions (black trace). Responses simulated with the model presented in the Appendix (red and blue). Parameter values: A = 2.9 s^{-2}, n_{cG} = 3, τ_E = 770 ms (determined with Pepperberg analysis from saturated flash responses in low Ca^{2+}, Vinberg & Koskelainen, 2010), τ_R = 70 ms in both simulations (red and blue). Red trace shows a simulated response with K_m = 100 μM, cG_{dark} = 32 μM and β_{dark} = 2.8 s^{-1}. Blue trace plots simulation with K_m = 10 μM, cG_{dark} = 21 μM and β_{dark} = 15 s^{-1}.

Aalto-ST 12/2011

ISBN: 978-952-60-4164-3 (pdf)
ISSN-L: 1799-4896
ISSN: 1799-490X (pdf)

Aalto University
School of Science
Department of Biomedical Engineering and Computational Science (BECS)
www.aalto.fi

BUSINESS + ECONOMY

ART + DESIGN + ARCHITECTURE

SCIENCE + TECHNOLOGY

CROSSOVER

DOCTORAL DISSERTATIONS